MYCOTAXON

ISSN (print) 0093-4666 (online) 2154-8889 Mycotaxon, Ltd. ©2022

April–June 2022—Volume 137, pp. 261–270

https://doi.org/10.5248/137.261

Adustochaete yunnanensis sp. nov. from China

Yi-Fei Li[1,3] & Chang-Lin Zhao[1,2,3,4*]

[1] *Yunnan Key Laboratory of Plateau Wetland Conservation, Restoration and Ecological Services,*
[2] *Key Laboratory for Forest Resources Conservation and Utilization in the Southwest Mountains of China, Ministry of Education,* and [3] *College of Biodiversity Conservation, Southwest Forestry University, Kunming 650224, P.R. China*
[4] *Yunnan Key Laboratory for Fungal Diversity and Green Development, Kunming Institute of Botany, Chinese Academy of Science, Kunming 650201, China*

* Correspondence to: *fungi@swfu.edu.cn*

Abstract—A new wood-rotting fungal species, *Adustochaete yunnanensis*, is described from China on the basis of morphological and molecular data. The new fungus is characterized by annual, resupinate basidiomata with a grandinioid hymenial surface, encrusted hyphidia, and narrow cylindrical to allantoid basidiospores. ITS and nLSU rRNA sequences were generated from samples and analyzed phylogenetically using Maximum Likelihood, Maximum Parsimony, and Bayesian Inference methods. The phylogeny clustered *A. yunnanensis* within *Adustochaete*, where it formed a well-supported independent lineage sister to a clade comprising *A. interrupta* and *A. rava*. An identification key to *Adustochaete* species is provided.

Key words—*Auriculariaceae, Auriculariales, Basidiomycota*, taxonomy, Yunnan Province

Introduction

The wood-rotting fungal genus *Adustochaete* Alvarenga & K.H. Larss., typified by *A. rava* Alvarenga & K.H. Larss., is characterized by small dry soft resupinate grayish to brownish basidiomata with spiny or tuberculate hymenophore; a monomitic hyphal system of generative hyphae with clamp connections; the presence of hyphidia and cystidia; basidia that are ellipsoid-ovoid to obconical, longitudinally septate, 4-celled, and occasionally tapering

to the stalk-like base; and hyaline, thin-walled, cylindrical to broadly cylindrical, straight or curved basidiospores containing oil droplets in the cytoplasm (Alvarenga & al. 2019). *Adustochaete* species are primarily wood decomposers, causing white-rot of angiosperms (Alvarenga & al. 2019) with characters similar to other white-rot fungi (Ma & al. 2019, Zhao & Ma 2019, Chen & al. 2020, Huang & al. 2020, Peng & Zhao 2020). Presently three species are accepted in this genus (Alvarenga & al. 2019, Hyde & al. 2020).

Alvarenga & al. (2019), who conducted comprehensive phylogenetic research on *Heterochaete* sensu lato (*Auriculariales*, *Basidiomycota*), proposed a new genus *Adustochaete*, which formed a single clade and grouped with *Eichleriella* Bres. and *Proterochaete* Spirin & V. Malysheva. The rDNA sequence analyses by Hyde & al. (2020) of all three *Adustochaete* species grouped *A. interrupta* Spirin & V. Malysheva, *A. nivea* Alvarenga, and *A. rava* in a single clade among clades of twelve other genera within *Auriculariaceae.*

During the investigations on wood-rotting fungi in southern China, an undescribed taxon was encountered. Analyses of the morphology and internal transcribed spacer (ITS) and large subunit nuclear ribosomal RNA gene (nLSU) sequences placed the unknown taxon in *Adustochaete*, where it is proposed here as a new species, *A. yunnanensis*.

Table 1. Species, specimens, and sequences used in this study (new sequences in bold).

Species	Sample	GenBank accession no.		Reference
		ITS	nLSU	
Adustochaete interrupta	LR 23435	MK391518	MK391527	Alvarenga & al. 2019
A. rava	RC 841	MK391516	—	Alvarenga & al. 2019
	KHL 15526	MK391517	MK391526	Alvarenga & al. 2019
A. yunnanensis	**CLZhao 8212 [T]**	MZ911964	MZ950629	Present study
	CLZhao 4671	MZ911965	—	Present study
	CLZhao 4401	MZ911966	MZ950630	Present study
Amphistereum leveilleanum	LentzFP 106715	KX262119	KX262168	Malysheva & Spirin 2017
A. schrenkii	Burdsall 8476	KX262130	KX262178	Malysheva & Spirin 2017
Aporpium caryae	Miettinen 14774	JX044145	JX044145	Miettinen & al. 2012
	WD 2207	AB871751	AB871730	Sotome & al. 2014
Auricularia mesenterica	Oberwinkler 25132	AF291271	AF291292	Wei & Oberwinkler 2001

A. polytricha	TUFC 12920	AB871752	AB871733	Sotome & al. 2014
Bourdotia galzinii	Miettinen 15900.4	MG757511	MG757511	Spirin & al. 2019
Ductifera sucina	Wells 2155	AY509551	AY509551	Spirin & al. 2019
Eichleriella crocata	TAAM 101077	KX262100	KX262147	Malysheva & Spirin 2017
E. tenuicula	ValCB 1	MK391515	MK391525	Alvarenga & al. 2019
Elmerina cladophora	Miettinen 14314	MG757509	MG757509	Spirin & al. 2019
E. sclerodontia	Miettinen 16431	MG757512	MG757512	Spirin & al. 2019
Exidia glandulosa	YC Dai 21232	MT663362	MT664781	Wu & al. 2020
	YC Dai 21233	MT663363	MT664782	Wu & al. 2020
Grammatus labyrinthinus	Yuan 1759	KM379137	KM379138	Alvarenga & al. 2019
	Yuan 1600	KM379139	KM379140	Alvarenga & al. 2019
Heterochaetella brachyspora	RJB 13295	AY509552	AY509552	Alvarenga & al. 2019
Heteroradulum kmetii	Ginns 2529	KX262135	KX262183	Malysheva & Spirin 2017
	Spirin 6466	KX262104	KX262152	Malysheva & Spirin 2017
Hyalodon piceicola	Spirin 2689	MG735414	MG735422	Spirin & al. 2019
	Spirin 11063	MG735415	MG735423	Spirin & al. 2019
Proterochaete adusta	CNOM 10519	MK391519	—	Alvarenga & al. 2019
	VS 9021	MK391520	MK391528	Alvarenga & al. 2019
Protodaedalea foliacea	Miettinen 13054	MG757507	MG757507	Spirin & al. 2019
Protodontia subgelatinosa	voucher 11079	MG735412	MG735420	Spirin & al. 2019
Protohydnum cartilagineum	SP 467240	MG735426	MG735419	Spirin & al. 2019
Protomerulius subreflexus	X 1593	MG757508	MG757508	Spirin & al. 2019
Pseudohydnum gelatinosum	—	AF384861	AF384861	Alvarenga & al. 2019
	AFTOL-ID 1875	DQ520094	DQ520094	Alvarenga & al. 2019
Sclerotrema griseobrunnea	Spirin 7674	KX262140	KX857818	Malysheva & Spirin 2017
	Niemelä 2722	KX262144	KX262192	Malysheva & Spirin 2017
Sistotrema brinkmannii	isolate 236	JX535169	JX535170	Grum-Grzhimaylo & al. 2018
Stypella vermiformis	Spirin 11330	MG735417	MG735425	Spirin & al. 2019
	OF 188059	MG735418	—	Spirin & al. 2019
Tremellochaete japonica	LE 303446	KX262110	KX262160	Malysheva & Spirin 2017
	TAA 42689	AF291274	AF291320	Wei & Oberwinkler 2001
Tremiscus helvelloides	AFTOL-ID 1680	DQ520100	DQ520100	Alvarenga & al. 2019

Materials & methods

The studied specimens have been deposited at the herbarium of Southwest Forestry University, Kunming, Yunnan Province, P.R. China (SWFC). Macromorphological descriptions are based on field notes. Colour terms follow Petersen (1996). The dried specimens were observed under a light microscope following Dai (2012). The following abbreviations are used: KOH = 5% potassium hydroxide, CB = Cotton Blue, CB– = acyanophilous, IKI = Melzer's reagent, IKI– = both non-amyloid and non-dextrinoid, L = mean spore length (arithmetic average of all spores), W = mean spore width (arithmetic average of all spores), Q = variation in the L/W ratios among specimens, and n = number of spores measured/number of specimens.

Genomic DNA was obtained from dried specimens using a CTAB rapid plant genome extraction kit-DN14 (Aidlab Biotechnologies Co., Ltd) following the manufacturer's instructions. The ITS region was amplified with primer pairs ITS5 and ITS4 (White & al. 1990), and the nLSU region was amplified with primer pairs LR0R and LR7 (http://lutzonilab.org/nuclear-ribosomal-dna). The PCR procedure for ITS was initial denaturation at 95 °C for 3 min, followed by 35 cycles at 94 °C for 40 s, 58 °C for 45 s, and 72 °C for 1 min, and a final extension of 72 °C for 10 min. The PCR procedure for nLSU was initial denaturation at 94 °C for 1 min, followed by 35 cycles at 94 °C for 30 s, 48 °C for 1 min, and 72 °C for 1.5 min, and a final extension of 72 °C for 10 min. The PCR products were purified and directly sequenced at Kunming Tsingke Biological Technology Limited Company (P.R. China). All newly generated sequences were deposited at GenBank (Table 1).

Sequencher 4.6 (GeneCodes) was used to edit the DNA sequences. Sequences were aligned in MAFFT v. 7 (https://mafft.cbrc.jp/alignment/server/) using the "G-INS-I" strategy and manually adjusted in BioEdit (Hall 1999). The sequence alignment was deposited in TreeBase (submission ID 28753). *Sistotrema brinkmannii* (Bres.) J. Erikss. was used as outgroup to root tree following Alvarenga & al. (2019) in the ITS+nLSU analyses (Fig. 1).

Maximum Parsimony (MP) analysis was applied to the ITS+nLSU dataset sequences. Approaches to phylogenetic analysis followed Zhao & Wu (2017), and the tree construction procedure was performed in PAUP* version 4.0b10 (Swofford 2002). All characters were equally weighted and gaps were treated as missing data. Trees were inferred using the heuristic search option with TBR branch swapping and 1000 random sequence additions. Max-trees were set to 5000, branches of zero length were collapsed and all parsimonious trees were saved. Clade robustness was assessed using a bootstrap (BT) analysis with 1000 replicates (Felsenstein 1985). Descriptive tree statistics tree length (TL), consistency index (CI), retention index (RI), rescaled consistency index (RC), and homoplasy index (HI) were calculated for each MP Tree generated. Sequences were also analyzed using Maximum Likelihood (ML) with RAxML-HPC2 through the Cipres Science Gateway (www.phylo.org, Miller & al. 2009). Branch support (BS) for ML analysis was determined by 1000 bootstrap replicates.

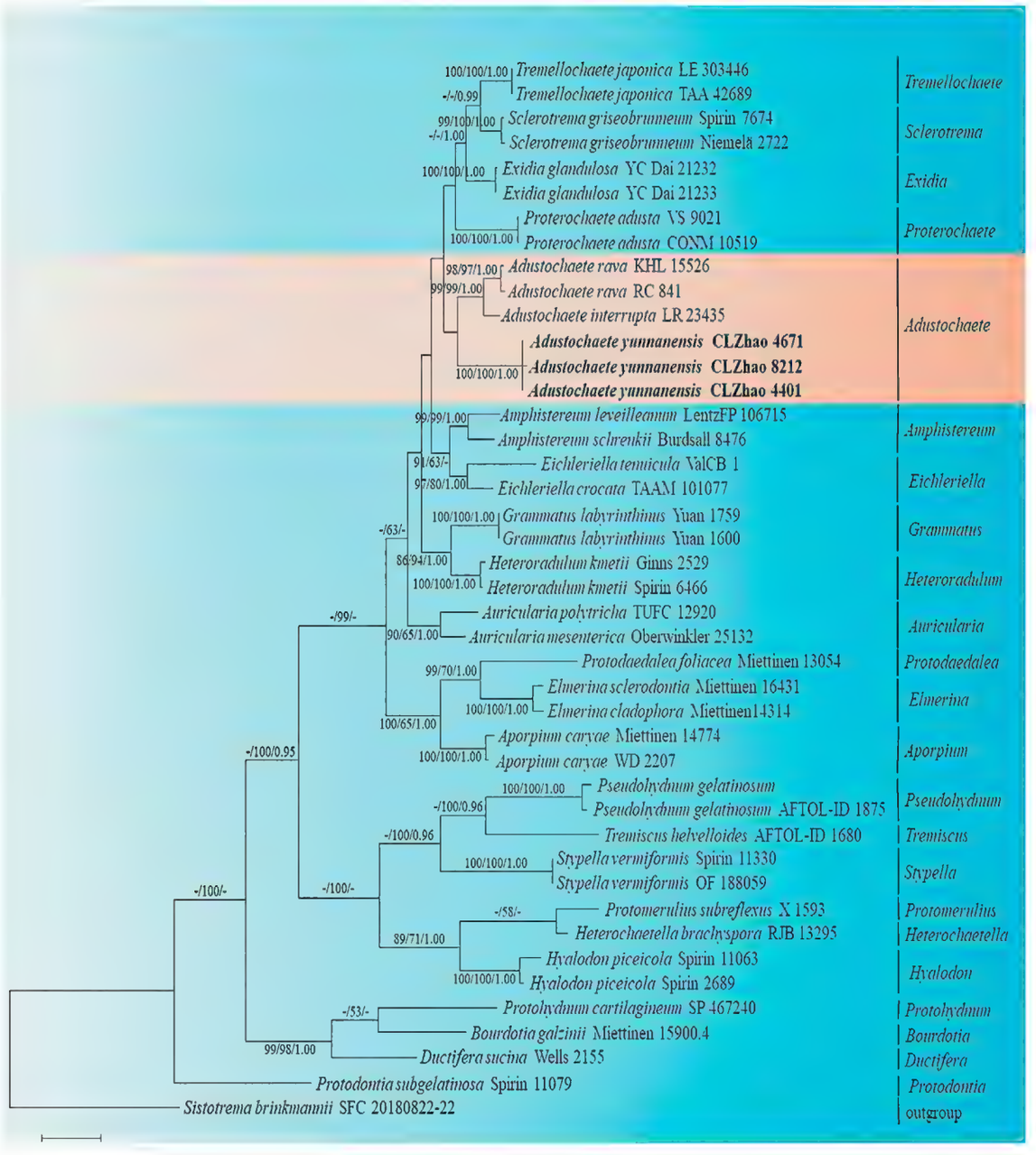

Fig. 1. Maximum parsimony strict consensus tree illustrating the phylogeny of *Adustochaete yunnanensis* and related genera in *Auriculariaceae*, based on ITS+nLSU sequences. Branches are labelled with maximum likelihood bootstrap values >70%, parsimony bootstrap values >50%, and Bayesian posterior probabilities >0.95.

MrModeltest 2.3 (Nylander 2004) was used to determine the best-fit evolution model for each data set for Bayesian Inference (BI). BI was calculated with MrBayes 3.1.2 with a general time reversible (GTR+I+G) model of DNA substitution using a Bayesian Posterior Probabilities (BPP) and a gamma distribution rate variation across sites (Ronquist & Huelsenbeck 2003). Four Markov chains run for 2 runs from random starting trees for 460 thousand generations and trees were sampled every 100 generations. The first one-fourth generations were discarded as burn-in.

A majority rule consensus tree of all remaining trees was calculated. Branches were considered as significantly supported if they received BS >70%, BT >50%, or BPP >0.95.

Molecular phylogeny

The ITS+nLSU dataset (Fig. 1) included sequences from 43 fungal specimens representing 30 taxa. The dataset had an aligned length of 2802 characters, of which 1260 characters were constant, 205 parsimony-uninformative, and 526 parsimony-informative. MP analysis yielded 1 equally parsimonious tree (TL = 280, CI = 0.440, HI = 0.560, RI = 0.533, RC = 0.234). The best-fit model for ITS+nLSU alignment estimated and applied in the BI was GTR+I+G, lset nst = 6, rates = invgamma; prset statefreqpr = dirichlet (1,1,1,1). BI produced a similar topology with an average standard deviation of split frequencies = 0.009507.

The phylogenetic tree inferred from ITS+nLSU sequences includes three *Adustochaete* species. The new taxon, *A. yunnanensis*, formed a well-supported lineage and was sister to a clade comprising *A. interrupta* and *A. rava* with lower support.

Taxonomy

Adustochaete yunnanensis C.L. Zhao, **sp. nov.** Figs 2, 3

MB 841453

Differs from *Adustochaete interrupta* by its grandinioid hymenial surface and larger basidiospores.

Holotype: China. Yunnan Province: Yuxi, Xingping County, Tea Horse Ancient Road spot, on the fallen angiosperm branch, 21 Aug 2018, CLZhao 8212 (**Holotype**, SWFC 008212; GenBank MZ911964, MZ950629).

Etymology: *yunnanensis* (Lat.) refers to the province locality of the type specimen.

Basidiomata annual, resupinate, soft, waxy, without odor or taste when fresh, becoming hard membranous on drying, ≤7 × 3 cm (length × breadth), ≤200 μm thick. Hymenial surface grandinioid, aculei 4–9 per mm, 40–135 μm long, grayish to pale brownish when fresh, turning dark grayish to brownish upon drying. Margin sterile, grayish, ≤1 mm wide.

Hyphal structure monomitic; hyphae generative, clamped, hyaline, more or less interwoven, thin-walled, frequently branched, 2–3 μm in diameter; IKI–, CB–; tissues unchanged in KOH.

Hymenium cystidia numerous, clavate to fusiform, hyaline, thin-walled, smooth, 17.5–24.5 × 3.5–5.8 μm, cystidioles absent; hyphidia abundant, variably branched, hyaline, thin-walled, encrusted with crystals at the apex, 19.5–30 × 4.5–8 μm; basidia narrowly ovoid to obconical, 4-celled, occasionally bearing an enucleate stalk, 25–47.5 × 8.5–14 μm; basidioles dominant, in shape similar to basidia, but slightly smaller.

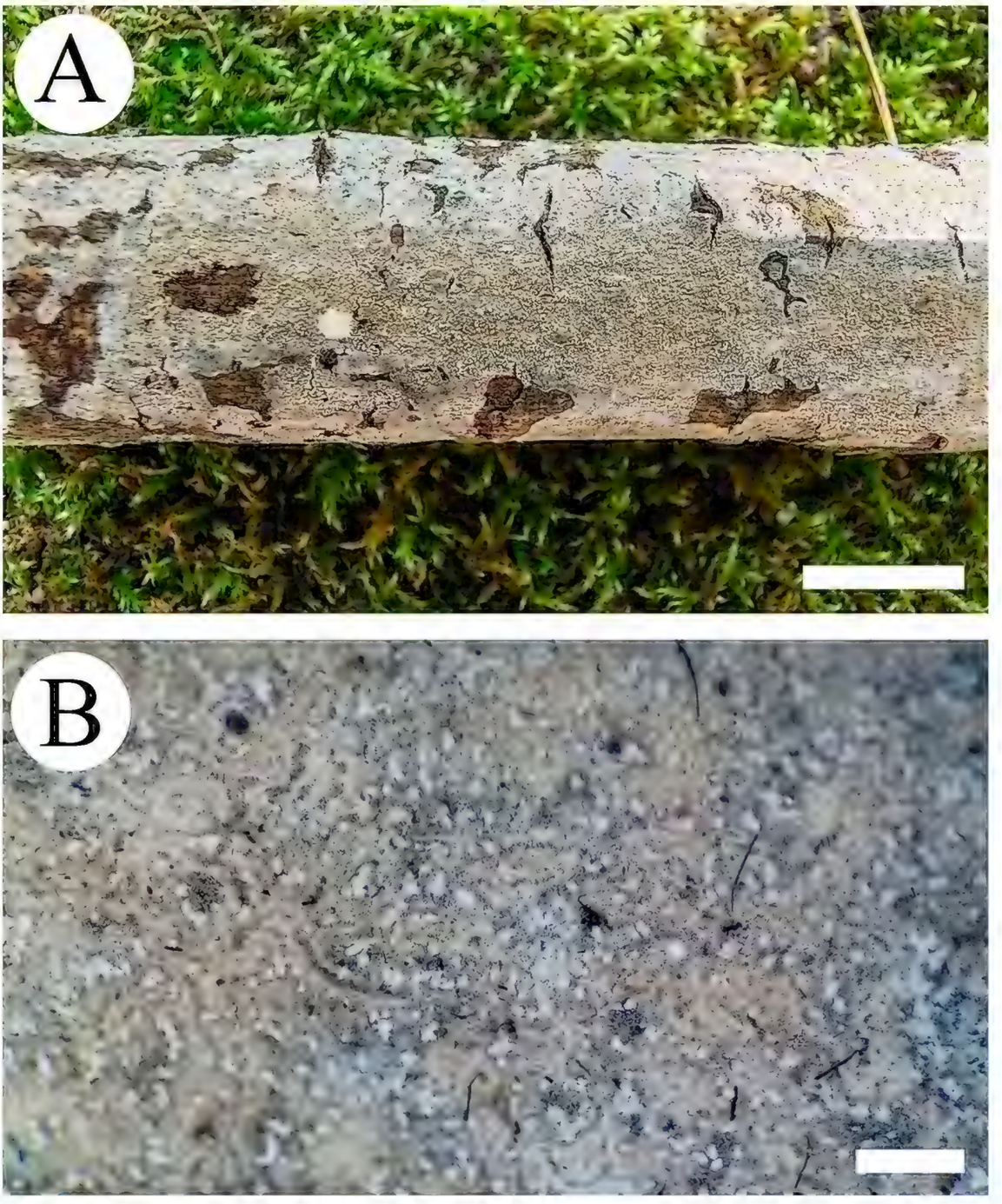

Fig. 2. *Adustochaete yunnanensis* (holotype, SWFC 008212).
A. Habit; B. Characteristic hymenophore. Scale bars A = 1 cm; B = 1 mm.

Basidiospores narrow cylindrical to allantoid, slightly to distinctly curved, hyaline, thin-walled, smooth, with oil droplets in the cytoplasm, IKI–, CB–, (11–)12–20(–21) × (4.5–)5–7(–7.5) μm, L = 15.5 μm, W = 5.7 μm, Q = 2.48–2.98 (n = 90/3).

Type of rot: white rot.

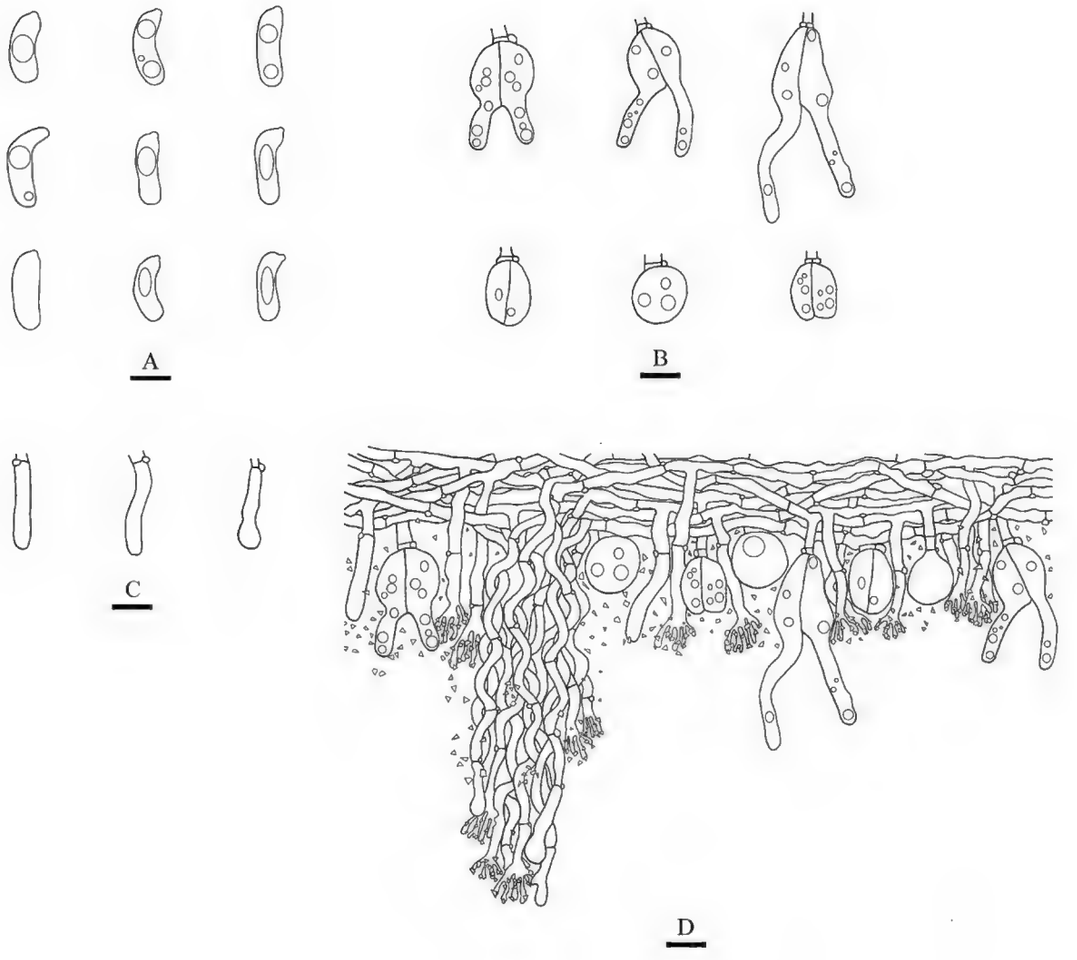

Fig. 3. *Adustochaete yunnanensis* (ex holotype, SWFC 008212).
A. Basidiospores; B. Basidia and basidioles; C. Cystidia; D. Section of hymenium.
Scale bars = 10 μm.

Additional specimens examined: **CHINA. Yunnan province. Puer:** Jingdong County, Wuliangshan National Nature Reserve, on a thick angiosperm branch, 6 Oct 2017, CLZhao 4671 (SWFC 004671; GenBank MZ911965); CLZhao 4401 (SWFC 004401; GenBank MZ911966, MZ950630).

Discussion

The previous morphological and molecular analyses by Alvarenga & al. (2019) strongly supported *Adustochaete* as an independent genus. In our ITS and nLSU sequence analyses, *A. yunnanensis* formed a well-supported monophyletic lineage sister to the *A. interrupta* + *A. rava* clade.

Adustochaete interrupta differs morphologically from *A. yunnanensis* in its light ochraceous-gray to brownish hymenophore, smaller basidia (15.1–24 ×

9.1–11.8 µm), and larger cystidia (45–96 × 6–13.5 µm, Alvarenga & al. 2019), and *A. rava* differs in its white, arachnoid to fimbriate margin, shorter basidia (10.8–15.2 × 7.3–10 µm), and longer cystidia (27–52 × 4–8 µm, Alvarenga & al. 2019). *Adustochaete nivea* differs from *A. yunnanensis* by having a white hymenial surface, smaller basidia (14.9–16.2 × 9.7–10.1 µm), and absence of cystidia (Hyde & al. 2020).

This the first report of an *Adustochaete* species in China (Wu & al. 2020).

Key to the four accepted species of *Adustochaete* worldwide

1. Cystidia absent ..... *A. nivea*
1. Cystidia present 2
2. Cystidia >25 µm long, basidia <24 µm long 3
2. Cystidia <25 µm long, basidia >24 µm long ..... *A. yunnanensis*
3. Basidia <15 µm long, basidiospores <5µm wide ..... *A. rava*
3. Basidia >15 µm long, basidiospores >5µm wide ..... *A. interrupta*

Acknowledgments

Special thanks are due to Drs. Mei-Ling Han (Langfang Normal University, Hebei, P.R. China) and Sana Jabeen (University of Education, Lahore, Pakistan) for expert presubmission review. The research was supported by the National Natural Science Foundation of China (Project No. 32170004), Yunnan Fundamental Research Project (Grant No. 202001AS070043), the High-level Talents Program of Yunnan Province (YNQRQNRC-2018-111), Yunnan Key Laboratory of Plateau Wetland Conservation, Restoration and Ecological Services (202105AG070002), and Science and Technology Innovation Project of Southwest Forestry University (KY21017).

Literature cited

Alvarenga RLM, Spirin V, Malysheva V, Gibertoni TB, Larsson KH. 2019. Two new genera and six other novelties in *Heterochaete* sensu lato (*Auriculariales*, *Basidiomycota*). Botany 97: 439–451. https://doi.org/10.1139/cjb-2019-0046

Chen JZ, Yang X, Zhao CL. 2020. *Vanderbylia cinnamomea* sp. nov. from southwestern China. Mycotaxon 135: 371–382. https://doi.org/10.5248/135.371

Dai YC. 2012. Polypore diversity in China with an annotated checklist of Chinese polypores. Mycoscience 53: 49–80. https://doi.org/10.1007/s10267-011-0134-3

Felsenstein J. 1985. Confidence intervals on phylogenetics: an approach using bootstrap. Evolution 39: 783–791. https://doi.org/10.1111/j.1558-5646.1985.tb00420.x

Grum-Grzhimaylo OA, Debets AJM, Bilanenko EN. 2018. Mosaic structure of the fungal community in the Kislo-Sladkoe Lake that is detaching from the White Sea. Polar Biology 41: 2075–2089. https://doi.org/10.1007/s00300-018-2347-9

Hall TA. 1999. BioEdit: a user-friendly biological sequence alignment editor and analysis program for Windows 95/98/NT. Nucleic Acids Symposium Series 41: 95–98. https://doi.org/10.1021/bk-1999-0734.ch008

Huang RX, Luo KY, Ma RX, Zhao CL. 2020. Morphological and molecular identification of *Phlebia wuliangshanensis* sp. nov. in China. Mycotaxon 135: 103–117. https://doi.org/10.5248/135.103

Hyde KD, Dong Y, Phookamsak R, Jeewon R, Bhat DJ, Jones EBG, Liu NG & al. 2020. Fungal diversity notes 1151–1276: taxonomic and phylogenetic contributions on genera and species of fungal taxa. Fungal Diversity 100: 5–277. https://doi.org/10.1007/s13225-020-00439-5

Ma RL, Gao M, Zhuang XL, Zhao CL. 2019. *Septobasidium aquilariae* sp. nov. from China. Mycotaxon 134: 517–528. https://doi.org/10.5248/134.517

Malysheva V, Spirin V. 2017. Taxonomy and phylogeny of the *Auriculariales* (*Agaricomycetes*, *Basidiomycota*) with stereoid basidiocarps. Fungal Biology 121: 689–715. https://doi.org/10.1016/j.funbio.2017.05.001

Miettinen O, Spirin V, Niemelä T. 2012. Notes on the genus *Aporpium* (*Auriculariales*, *Basidiomycota*), with a new species from temperate Europe. Annales Botanici Fennici 49: 359–368. https://doi.org/10.5735/085.049.0607

Miller MA, Holder MT, Vos R, Midford PE, Liebowitz T, Chan L, Hoover P, Warnow T. 2009. The CIPRES Portals. CIPRES url: http://www.phylo.org/sub_sections/portal. 2009-08-04. (Archived by WebCite® at https://www.webcitation.org/5imQlJeQa).

Nylander JAA. 2004. MrModeltest v2. Program distributed by the author. Evolutionary Biology Centre, Uppsala University, Uppsala.

Peng JH, Zhao CL. 2020. *Armillaria xiaocaobaensis* sp. nov. from China. Mycotaxon 135: 431–441. https://doi.org/10.5248/135.431

Ronquist F, Huelsenbeck JP. 2003. MrBayes 3: Bayesian phylogenetic inference under mixed models. Bioinformatics 19: 1572–1574. https://doi.org/10.1093/bioinformatics/btg180

Sotome K, Maekawa N, Nakagiri A, Lee SS, Hattori T. 2014. Taxonomic study of Asian species of poroid *Auriculariales*. Mycological Progress 13: 987–997. https://doi.org/10.1007/s11557-014-0984-0

Spirin V, Malysheva V, Miettinen O, Vlasák J, Alvarenga RLM, Gibertoni TB, Ryvarden L, Larsson KH. 2019. On *Protomerulius* and *Heterochaetella* (*Auriculariales*, *Basidiomycota*). Mycological Progress 18: 1079–1099. https://doi.org/10.1007/s11557-019-01507-0

Swofford DL. 2002. PAUP*: phylogenetic analysis using parsimony (*and other methods). Version 4.0b10. Massachusetts: Sinauer Associates.

Wei M, Oberwinkler F. 2001. Phylogenetic relationships in *Auriculariales* and related groups – hypotheses derived from nuclear ribosomal DNA sequences. Mycological Research 105: 403–415. https://doi.org/10.1017/S095375620100363X

White TJ, Bruns TD, Lee SB, Taylor JW. 1990. Amplification and direct sequencing of fungal ribosomal RNA genes for phylogenetics. 315–322, in: MA Innis & al. (eds). PCR protocols: a guide to methods and applications. Academic Press, New York. https://doi.org/10.1016/B978-0-12-372180-8.50042-1

Wu F, Zhao Q, Yang ZL, Ye SY, Rivoire B, Dai YC. 2020. *Exidia yadongensis*, a new edible species from East Asia. Mycosystema 39: 1203–1214. https://doi.org/10.13346/j.mycosystema.200205

Zhao CL, Ma X. 2019. *Perenniporia mopanshanensis* sp. nov. from China. Mycotaxon 134: 125–137. https://doi.org/10.5248/134.125

Zhao CL, Wu ZQ. 2017. *Ceriporiopsis kunmingensis* sp. nov. (*Polyporales*, *Basidiomycota*) evidenced by morphological characters and phylogenetic analysis. Mycological Progress 16: 93–100. https://doi.org/10.1007/s11557-016-1259-8